

Optimized Passive Dynamics Improve Transparency of Haptic Devices

Heike Vallery *Member, IEEE*, Alexander Duschau-Wicke *Graduate Student Member, IEEE*,
and Robert Riener *Member, IEEE*

Abstract—For haptic devices, compensation of the robot’s gravity is a frequent strategy with the aim to reduce interaction forces between robot and human in zero-impedance control. However, a closer look at the composition of these interaction forces may reveal that the net effect of uncompensated gravitational components of the robot actually reduces interaction forces during dynamic movements, because inertial and gravitational components at least partially compensate each other. This is the case in lower extremity exoskeletons, where less user force is necessary to swing the robot’s leg when gravity helps. Here, we go one step further by shaping optimal passive dynamics for arbitrary haptic devices. The proposed method of *Generalized Elasticities* uses conservative force fields to improve haptic transparency for certain movements types. In an example realization, these force fields are generated by elasticities spanning multiple joints. Practical experiments with the Lokomat lower extremity exoskeleton show the success of the proposed method in terms of reduced interaction torques and more physiological user motion compared to gravity compensation.

I. INTRODUCTION

Over the last years, robots are coming ever closer to humans. An example of such close proximity are haptic devices. A common issue in most haptic devices is the question of how to enable good zero impedance, i.e. how to render the device as transparent as possible.

One of the most effective possibilities of achieving high transparency is by minimizing mass of the mechanical design, like in the commercially available PHANTOM device (SensAble Technologies, Inc.). However, mass reduction is limited when a certain force and power are needed. Especially devices that aim to assist human motion need to be capable of generating high forces. The purpose and kinematics of assistive devices varies. A frequent realization are exoskeletons (powered orthotic devices) for motor impaired patients, both for upper [1], [2] and lower extremities [3]–[7]. Besides exoskeletons, there are other kinematic concepts like end-effector training robots that are coupled only to the subject’s hand [8], feet [9], [10], or to the hip [11]. Also devices with the more general aim of enhancing physical capabilities have been developed [12], [13], for example to allow carrying of heavy loads. Although these devices aim to assist human motion, zero impedance is an important subordinate control feature. This does not only apply for healthy subjects, but also for rehabilitation scenarios. Recent control strategies for rehabilitation robots aim to increase

active patient participation to improve training efficacy [14]. With zero-impedance control as the basis, assistive forces are added only when needed [15]. In special cases, the intention of the user can be estimated, this allows to control the exoskeleton accordingly and achieve good transparency. The intention can for example be measured using EMG [12], [16] or by close observation of residual body motion [17]. However, in most haptic devices, no on-line information on the human’s motion intention is available.

Transparency can be improved by use of compliant actuation [18], which at least reduces inertial forces generated by the actuators. However, it is difficult to avoid additional mass after the actuators (e.g. due to an end-effector). Furthermore, compliant concepts require a compromise concerning achievable maximum stiffness [19], which might be needed for other tasks of the robot (like high-precision position control).

Closed-loop force control, for example using impedance or admittance control concepts, is an efficient means to improve transparency, because it can reduce the reflected inertia of the robot and its actuators [20]–[22]. However, this reduction is limited, and there will always be inertial forces remaining [21]. Furthermore, force sensors are required.

As reduction of inertia is limited, a common attempt to further reduce interaction forces is to compensate “at least” gravity of the robot (and possibly Coriolis and friction forces, which are mostly smaller). Though this seems intuitive, it is based on the implicit supposition that the magnitude of interaction forces depends on the *sum of absolute values* of inertial and gravitational terms. For some scenarios, this is true: In slow movements, inertial forces are small, and gravity compensation improves transparency. However, there are many applications where movements are dynamic, and where gravity compensation is not beneficial. During walking for example, interaction forces caused by an exoskeleton can even *increase* due to gravity compensation. For the LOPES gait rehabilitation robot [3], it was reported that the device is more transparent without gravity compensation, due to a similar eigenfrequency of robotic and human legs. With the help of gravity, human and robot legs swing in parallel while exchanging hardly any forces.

The example shows that it can be beneficial to shape passive dynamics of a haptic device, which are in this case similar to the human’s passive dynamics. An explanation is that the human motor system exploits natural dynamics in a very efficient manner, for example by swinging the legs during walking. In general, human movements match theoretical predictions of models optimized for various efficiency criteria [23]. Therefore, when passive dynamics of the human

All authors are with the Sensory-Motor Systems Lab, Institute of Robotics and Intelligent Systems, ETH Zurich, Zurich, Switzerland, and with the Spinal Cord Injury Center, University Hospital Balgrist, Zurich. A. Duschau-Wicke is also with Hocoma AG, Volketswil, Switzerland. hvallery@ethz.ch, riener@mavt.ethz.ch, alexander.duschau-wicke@hocoma.ch

body are transferred to a robot that moves similar to a human, energy expenditure to move the robot is minimized *implicitly*. Therefore, such a procedure has been suggested both for autonomous robots and for exoskeletons. In contrast to the first biped robots, which needed high power requirements to execute Computed-Torque-based position control, passive dynamic or ballistic walkers (e.g. [24]) exploit natural limb frequencies and enable natural-looking gait with minimal energy. For exoskeletons, Ferris [25] suggested to emulate passive joint elasticities, departing from the observation that the human Achilles tendon stores a large amount of energy during walking. A theoretical study also stressed the benefit of extra elastic elements on the human body using so-called *exotendons*, which van den Bogert [26] virtually attached to the human body in simulations. He showed that this may lead to a dramatic reduction of energy expenditure.

In this paper, we show how passive dynamics for general haptic devices can be optimized explicitly using the concept of *Generalized Elasticities*. The approach aims at minimizing interaction forces between human and robot, given that the user's preferred movements are approximately known in advance. Generalized Elasticities are based on optimal conservative force fields. No model of the human is needed for this algorithm, and the robot's kinematic structure does not have to resemble that of the human limbs. In practical experiments with the Lokomat exoskeleton [5], interaction torques with Generalized Elasticities (combined with closed-loop force control) are compared to closed-loop force control without additional feedforward terms, and to closed-loop force control with gravity compensation.

II. GENERALIZED ELASTICITIES

A. Problem Statement

We consider an arbitrary robot that is to be moved by a human, whereby interaction forces/torques¹ are to be minimized via control. We assume that the motion of the robot can be described in terms of the coordinates \mathbf{q} . The inertia of the robotic manipulator and its actuators are subsumed in a common mass matrix $\mathbf{M}_r(\mathbf{q})$. Gravitational, damping, and Coriolis torques are subsumed in $\mathbf{n}_r(\mathbf{q}, \dot{\mathbf{q}})$. With these conventions, the robot's equations of motion are:

$$\boldsymbol{\tau}_{\text{need}}(\mathbf{q}, \dot{\mathbf{q}}, \ddot{\mathbf{q}}) = \mathbf{M}_r(\mathbf{q})\ddot{\mathbf{q}} + \mathbf{n}_r(\mathbf{q}, \dot{\mathbf{q}}). \quad (1)$$

The needed torques $\boldsymbol{\tau}_{\text{need}}$ to move the robot can be generated by the robot's actuators or by the human. Forces from the human acting on the robot are the interaction torques $\boldsymbol{\tau}_{\text{int}}$, and actuator torques are written as $\boldsymbol{\tau}_{\text{act}}$:

$$\boldsymbol{\tau}_{\text{need}} = \boldsymbol{\tau}_{\text{int}} + \boldsymbol{\tau}_{\text{act}}. \quad (2)$$

The question is how we can find a control law for the robot's actuators such that they take over the main part, and that the torques that need to be generated by the human are minimal.

If the robot is equipped with force (or acceleration) sensors to measure (or estimate) $\boldsymbol{\tau}_{\text{int}}$ on-line, we assume that closed-loop force control is applied. However, there will always

¹Without loss of generality, only the term torques is used in the following.

be a certain minimum inertia remaining [21]. Therefore, in addition to feedback (fb) terms depending on force, also feedforward (ff) terms depending on time or position can be beneficial to make $\boldsymbol{\tau}_{\text{act}}$ match the needed torques closely:

$$\boldsymbol{\tau}_{\text{act}} = \boldsymbol{\tau}_{\text{fb}} + \boldsymbol{\tau}_{\text{ff}}. \quad (3)$$

We assume that $\boldsymbol{\tau}_{\text{fb}}$ reduces the mass matrix $\mathbf{M}_r(\mathbf{q})$ to the minimum achievable value using concepts like admittance or impedance control (and possibly $\mathbf{n}_r(\mathbf{q}, \dot{\mathbf{q}})$ is also modified, for example to compensate friction). Then, the equations of motion (1) are changed to:

$$\boldsymbol{\tau}_{\text{need}'}(\mathbf{q}, \dot{\mathbf{q}}, \ddot{\mathbf{q}}) = \mathbf{M}_{r'}\ddot{\mathbf{q}} + \mathbf{n}_{r'}(\mathbf{q}, \dot{\mathbf{q}}). \quad (4)$$

With (2) and (3), the residual needed torques are

$$\boldsymbol{\tau}_{\text{need}'} = \boldsymbol{\tau}_{\text{need}} - \boldsymbol{\tau}_{\text{fb}} = \boldsymbol{\tau}_{\text{int}} + \boldsymbol{\tau}_{\text{ff}}. \quad (5)$$

This representation includes the special case without closed-loop force control ($\boldsymbol{\tau}_{\text{fb}} = 0$), such that $\mathbf{M}_{r'} = \mathbf{M}_r$, and also the case where $\mathbf{n}_{r'} = \mathbf{n}_r$. A standard procedure would be to use $\boldsymbol{\tau}_{\text{ff}}$ as a function of \mathbf{q} for gravity cancellation. As outlined earlier, this is only optimal for certain movements, for example for very slow ones. The following sections describe the optimal design of feedforward components $\boldsymbol{\tau}_{\text{ff}}$ that are tailored optimally for arbitrary preferred user movements.

B. Minimizing Interaction by Conservative Force Fields

To minimize interaction torques, we will solve an optimization problem. No biomechanical model of the user is necessary, the only input needed for the optimization is a model of the robot and one or more movements the user prefers to perform. The robot's kinematic structure and mass distribution does not need to resemble that of the human body, which means that the approach can be used for exoskeletons and end-effector-based systems alike. The method uses conservative force fields, such that the robot emulates the behavior of passive components. Thus, no net energy is provided to the user, who has to initiate and control any motion. No force sensors are needed for its realization.

In order for $\boldsymbol{\tau}_{\text{ff}}$ to describe a conservative force field, its work must be zero for any closed trajectory. This implies that the torques in the vector $\boldsymbol{\tau}_{\text{ff}}$ can be interpreted as "elastic" functions of the joint variables \mathbf{q} , and as the negative gradient of a potential field $\phi(\mathbf{q})$ with respect to \mathbf{q} :

$$\boldsymbol{\tau}_{\text{ff}} = \boldsymbol{\tau}_{\text{elast}}(\mathbf{q}) = -\nabla_{\mathbf{q}}\phi(\mathbf{q}). \quad (6)$$

Apart from the conservativeness constraint, this representation is very open, such that it can for example represent elastic belts or even gravity cancellation.

The optimization procedure shapes the potential ϕ and thus $\boldsymbol{\tau}_{\text{elast}}$ as functions of \mathbf{q} in such a way that interaction torques needed to move the robot along given trajectories are minimal. Using (5) and (6), these residual interaction torques required to move the compensated robot are given by

$$\boldsymbol{\tau}_{\text{int}}(\mathbf{q}, \dot{\mathbf{q}}, \ddot{\mathbf{q}}) = \boldsymbol{\tau}_{\text{need}'}(\mathbf{q}, \dot{\mathbf{q}}, \ddot{\mathbf{q}}) - \boldsymbol{\tau}_{\text{elast}}(\mathbf{q}). \quad (7)$$

If a set of trajectories is given with n samples for \mathbf{q} and the corresponding velocities $\dot{\mathbf{q}}$ and accelerations $\ddot{\mathbf{q}}$, the goal is to minimize the quadratic cost function J with

$$J = \left\| \begin{pmatrix} \tau_{\text{need}'}(\mathbf{q}_1, \dot{\mathbf{q}}_1, \ddot{\mathbf{q}}_1) \\ \dots \\ \tau_{\text{need}'}(\mathbf{q}_k, \dot{\mathbf{q}}_k, \ddot{\mathbf{q}}_k) \\ \dots \\ \tau_{\text{need}'}(\mathbf{q}_n, \dot{\mathbf{q}}_n, \ddot{\mathbf{q}}_n) \end{pmatrix} - \begin{pmatrix} \tau_{\text{elast}}(\mathbf{q}_1) \\ \dots \\ \tau_{\text{elast}}(\mathbf{q}_k) \\ \dots \\ \tau_{\text{elast}}(\mathbf{q}_n) \end{pmatrix} \right\|_{\mathbf{Q}}^2, \quad (8)$$

whereby the symmetric positive definite matrix \mathbf{Q} contains weights that stress the importance of certain joints (Extreme weights might even increase interaction torques at one joint to transfer energy to others) and of certain instances k of the movement. Following (5), the needed torques are calculated using the robot model and expected trajectories with given positions, velocities and accelerations. The aim of the optimization is to find the optimal torques $\tau_{\text{elast}}(\mathbf{q})$ that compensate $\tau_{\text{need}'}(\mathbf{q}, \dot{\mathbf{q}}, \ddot{\mathbf{q}})$ for the expected motions and fulfill the constraint of conservativeness (6). It should be noted that it is *not* the aim to urge the human to perform the expected movement, like in impedance control. Nevertheless, when the movement differs strongly from the expected movement types, compensation is not optimal anymore, and interaction torques might increase.

For trivial problems, the optimal passive dynamics can be deduced intuitively. For example, we consider a one-dimensional robot represented by a floating point mass (no gravity acting), which a user moves in a sinusoidal oscillation. Here, the optimal passive position-dependent element to be added is a linear spring (with appropriate stiffness to achieve the desired eigenfrequency). Thus, the passive force field linearly depends on position, and it reduces necessary user interaction torques to maintain the oscillation to zero.

If the problem is not trivial, a suitable parameterization of the conservative force field $\tau_{\text{elast}}(\mathbf{q})$ can be set up, and the parameters need to be optimized. Such a parameterization can be done either in terms of the potential, or directly in terms of the force field. In the first place, an arbitrary C^1 -continuous scalar function of \mathbf{q} can be used. In the second case, the constraint of conservativeness must be considered, such that a possible strategy would be to build the force field by superimposing several passive elements. There is an almost infinite number of possible parameterizations, especially depending on the dimensionality of the problem. A frequent choice are polynomials or Radial Basis Functions (RBFs, see e.g. [27]). In the following, we parameterize the force field based on polynomials.

C. Example Force Field

To give an example how to parameterize the conservative force field $\tau_{\text{elast}}(\mathbf{q})$ in (6), a superposition of passive components is used, which are linear in their parameters and motivated by the idea of rubber belts spanning two joints (Fig. 1). The belt spanning joints j and j' with the levers r_j and $r_{j'}$ lengthens/shortens by s with

$$s = r_j q_j + r_{j'} q_{j'}. \quad (9)$$

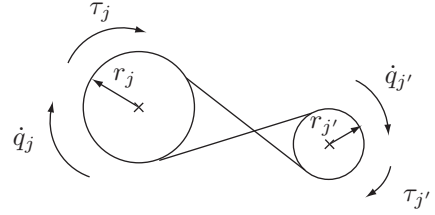


Fig. 1. Exemplary elasticity spanning a pair of joints j and j' , and the torques produced on each joint by the elasticity.

If the elasticity reacts to the deformation by a resulting force with magnitude $f(s)$, the torques on the two joints are

$$\tau_j = -r_j f(s) \quad (10)$$

$$\tau_{j'} = -r_{j'} f(s). \quad (11)$$

The lever $r_{j'}$ can be negative, such that s is a weighted difference of joint angles, or it can be zero, such that s is proportional to the value of q_j with respect to an inertial frame. This last case describes a single-joint elasticity, where no energy is transferred from one joint to another.

The idea of a “rubber belt” was meant for helping to visualize the structure, because the real resulting force f , as opposed to a force from a rubber belt, can be an arbitrary function of the deformation s , it does not necessarily increase or decrease monotonously. Furthermore, the joints need not be rotational, and s could be a weighted sum of more than two joints. More general, the deformation s_a of the a -th elasticity can be written in vector notation using the vector \mathbf{r}_a containing constant levers for each joint:

$$s_a := \mathbf{r}_a^T \mathbf{q}. \quad (12)$$

The joint torque vector $\tau_a(\mathbf{q})$ produced by the elasticity is

$$\tau_a(\mathbf{q}) := -\mathbf{r}_a f_a(s_a), \quad (13)$$

with an unknown scalar function $f_a(s_a)$ to be found via optimization. The previous example can be seen as a special case with all entries of \mathbf{r}_a set to zero except for two.

A force field designed by superposition of various of these “elastic belts” is intrinsically conservative, no work is performed along any closed path.

Proof: If a potential $\phi_a(\mathbf{q})$ of the a -th elasticity exists, according to (6) it must fulfill the conditions

$$\nabla_{\mathbf{q}} \phi_a = -\tau_a(\mathbf{q}). \quad (14)$$

With candidates chosen as the indefinite integral

$$\phi_a(\mathbf{q}) = \int f_a(s_a) ds_a, \quad (15)$$

the gradient is given by

$$\nabla_{\mathbf{q}} \phi_a = \nabla_{\mathbf{q}} s_a f_a(s_a). \quad (16)$$

With (12), this is

$$\nabla_{\mathbf{q}} \phi_a = \mathbf{r}_a f_a(s_a). \quad (17)$$

Due to (13), the condition (14) is fulfilled. As a sum of conservative force fields is again conservative, the superposition of elasticities describes a conservative force field. ■

A number l of such elasticities can now be designed by choosing various linear combinations of the joints. An intuitive approach is to chose always pairs of joints, as in

the example (There can be several elasticities spanning the same pair of joints with different levers). To simplify the optimization, linear functions f_a can be chosen with basis functions $g_{ai}(s_a)$ subsumed in the vector function $\mathbf{g}_a(s_a)$ and parameters p_{ai} subsumed in \mathbf{p}_a :

$$f_a(s_a) = \sum_{i=0}^v p_{ai} g_{ai}(s_a) = [\mathbf{g}_a(s_a)]^T \mathbf{p}_a. \quad (18)$$

Then, an overall matrix $\mathbf{R}(\mathbf{q})$ for all l elasticities with

$$\mathbf{R}(\mathbf{q}) := \begin{pmatrix} -r_1 \mathbf{g}_1^T & \dots & -r_a \mathbf{g}_a^T & \dots & -r_l \mathbf{g}_l^T \end{pmatrix} \quad (19)$$

and an overall parameter vector \mathbf{p} with

$$\mathbf{p} := (\mathbf{p}_1^T \quad \dots \quad \mathbf{p}_a^T \quad \dots \quad \mathbf{p}_l^T)^T \quad (20)$$

allow to write the torque vector $\boldsymbol{\tau}_{\text{elast}}(\mathbf{q})$ generated by all l elasticities τ_a in (13) for one specific position \mathbf{q} as

$$\boldsymbol{\tau}_{\text{elast}}(\mathbf{q}) = \sum_{a=1}^l \tau_a(\mathbf{q}) = \mathbf{R}(\mathbf{q}) \mathbf{p}. \quad (21)$$

Now, the optimization can be performed using the given preferred trajectories with in total n samples. When the matrices $\mathbf{R}(\mathbf{q}_k)$, with $k = 1 \dots n$, are concatenated to the matrix \mathbf{A} , and the vectors $\boldsymbol{\tau}_{\text{need}}'(\mathbf{q}_k, \dot{\mathbf{q}}_k, \ddot{\mathbf{q}}_k)$ are concatenated to a vector \mathbf{b} for all samples, the cost function of (8) is:

$$J = \|\mathbf{b} - \mathbf{A}\mathbf{p}\|_{\mathbf{Q}}^2 \quad (22)$$

This is a linear Least Squares (LS) problem and the parameter vector \mathbf{p} can be found recursively or by use of the pseudoinverse. An important fact is that the matrix \mathbf{A} might have deficient rank, because parameters are redundant. This can be avoided by additional constraints, for example by setting selected parameters p_{ai} to zero. If the number of parameters is not too high, the issue can also be solved by penalizing high values; for example diagonal matrices could be concatenated to \mathbf{A} and to \mathbf{Q} , and a zero vector to \mathbf{b} .

D. Application to the Lokomat robot

The Lokomat [5] is a robotic exoskeleton with two actuated Degrees of Freedom per leg: Hip and knee flexion/extension in the sagittal plane. It is equipped with a treadmill and a body weight support (BWS) system. Vertical motion of the robot is supported by a parallelogram structure with passive weight compensation. The robot's equations of motion (1) describe each leg as a double pendulum with added actuator inertia. The robot comprises force sensors between the actuators and the exoskeleton, such that reflected drive inertia can be reduced by force control. Using force control with the maximum possible gain, the reflected inertia of the device is still approximately 0.3 kgm^2 for the knee, and 1.4 kgm^2 for the hip in an average configuration. This is more than twice the corresponding inertia of the human limbs, and it is mainly due to the stiff actuators with high transmission ratio. This high inertia is the main cause of the interaction torques in dynamic gait.

In addition to the closed-loop force control, Generalized Elasticities are now designed for the robot to further reduce

interaction torques. To obtain the residual needed torques according to (5), the preferred motion of the human needs to be approximately known. Here, it helps that gait patterns of different healthy subjects are similar. An exemplary gait pattern has been taken from the public domain Carnegie Mellon Database². The angle trajectory \mathbf{q} contains four elements, corresponding to the robot's four DoFs. The derivatives $\dot{\mathbf{q}}$ and $\ddot{\mathbf{q}}$ are calculated using local polynomial approximation.

The parameterization of the conservative force field is done according to section II-C. To simplify the description, all functions $g_{ai}(s_a)$ in (18) are identical for all elasticities, and they are powers of s_a :

$$g_{ai}(s_a) = s_a^i, \quad a = 1, \dots, l, \quad i = 1, \dots, v. \quad (23)$$

Here, the degree v of the polynomial is chosen as seven (Such that each elasticity has eight parameters). For each joint j of the robot's four actuated joints, one single-joint elasticity a and two coupling elasticities b and c , each to one other joint, are designed, using transmission ratios $r_{j'}/r_j$ of 1 or -1. More specifically, $s_a = q_j$, $s_b = q_j + q_{j'}$, and $s_c = q_j - q_{j'}$. This leads to four single-joint elasticities, and eight more elasticities spanning two joints: Right hip/left hip, right knee/right hip, left knee/left hip, right knee/left knee. Because the robot is symmetric, and the force field should also be symmetric, the parameters of corresponding elasticities are constrained to be equal. This reduces the size of the matrix \mathbf{R} , and the number of parameters decreases from $12 \cdot 8 = 96$ to $8 \cdot 8 = 64$. The matrix \mathbf{A} has deficient rank, and this is solved by concatenating a 64×64 diagonal matrix to penalize high coefficients. The matrix \mathbf{Q} is diagonal, and weightings for knee torques are larger compared to the hip by a factor of 10^4 . This is done in accordance with perception of subjects walking in the Lokomat, where knee interaction torques are perceived as being more severe than hip interaction torques. In other words, suboptimal compensation for the hip is tolerated in order to improve transparency for the knee. There is no weighting of specific instances in the gait cycle.

III. EXPERIMENTAL PROTOCOL AND DATA ANALYSIS

Eight healthy young subjects took part in the study (four female, four male), and each walked on a treadmill at 3 km/h with body weight support (effective body weight reduced by 30%, which is the standard procedure during clinical use of the Lokomat) under four different conditions:

- without the robot (condition 0, Free)
- with the robot, closed-loop force control without feed-forward compensation (condition 1, NoCmp)
- with the robot, closed-loop force control and Generalized Elasticities (condition 2, Elast)
- with the robot, closed-loop force control and compensation of gravity, Coriolis, and centrifugal torques of the robot's legs (condition 3, GrvCmp)

The conditions were randomized, and subjects walked three minutes with each controller, without being told which one

²<http://mocap.cs.cmu.edu>

was active. Prior to each condition, there was a rest of one minute standing in the robot. Joint torques and joint angles of the robot were recorded in conditions 1 to 3, as well as walking cadence, i.e. the number of single steps per minute. In condition 0, only walking cadence was measured.

A very direct criterion to evaluate the performance of each of the controllers are interaction torques. The robot's force sensors are located between drives and exoskeleton and not directly at the interaction points with the human, such that a model of the exoskeleton's dynamics has to be used. The given model allows for an acceptable reconstruction. Given the trajectory recorded during gait and smoothed numerical derivatives thereof, the interaction torques that the human had to provide to move the robot are calculated:

$$\tau_{\text{int}} = \mathbf{M}_{\text{exo}}(\mathbf{q})\ddot{\mathbf{q}} + \mathbf{n}_{\text{exo}}(\mathbf{q}, \dot{\mathbf{q}}) - \tau_{\text{sensors}}. \quad (24)$$

In contrast to \mathbf{M}_r in (4), only the inertia \mathbf{M}_{exo} of the exoskeleton needs to be used here and inertia of the drives is excluded due to the force sensor location. To quantify overall interaction torques, the root mean square of the interaction torques during the last minute ($T = 60$ s) was calculated for each joint j of the four joints (hip and knee of both legs). The average value

$$\bar{\tau}_{\text{int}} = \frac{1}{4} \sum_{j=1}^4 \sqrt{\frac{1}{T} \int_0^T [\tau_{\text{int},j}(t)]^2 dt} \quad (25)$$

is used as a measure of the interaction between robot and human under a particular condition.

A second performance criterion is the walking cadence, which provides a measure of how closely the subject matches his/her original gait pattern.

The different conditions were compared by a 1-way ANOVA at the 5% significance level. Multiple comparisons were accounted for by the Bonferroni adjustment.

IV. RESULTS

The average RMS interaction torques between robot and human show a significant difference between the three conditions in the robot (Fig. 2), although one subject did not complete all trials due to technical problems. Estimated means are 10.4, 7.9, and 14.8 N, in the order of controllers. Thus,

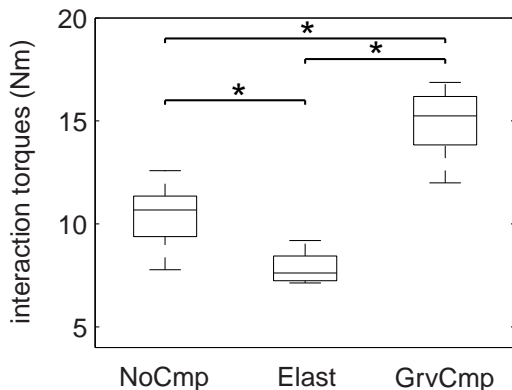


Fig. 2. Average RMS joint interaction torque $\bar{\tau}_{\text{int}}$ of all subjects ($n = 8$) for the different Lokomat conditions.

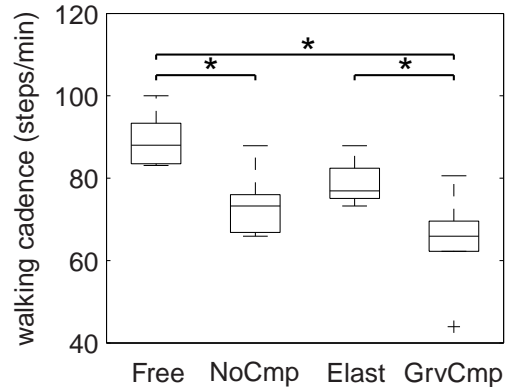


Fig. 3. Walking cadences of all subjects ($n = 8$) for free walking and the different Lokomat conditions.

the elasticities reduced average joint interaction torques by almost 50% compared to gravity compensation.

Concerning walking cadence, free walking differs significantly from all other conditions except for walking with Generalized Elasticities (Fig. 3). Furthermore, Generalized Elasticities differ significantly both from gravity compensation and from bare closed-loop force control.

As a negative effect of the Generalized Elasticities, several subjects remarked that the condition disturbed foot clearance in initial swing. The data showed high knee interaction torques almost exclusively in this phase (up to about 12 Nm extension torque), and of short duration. Maximum interaction torques were higher with the other conditions, but they built up more gradually.

V. DISCUSSION

The results show that gravity compensation of the exoskeleton legs is counterproductive during gait, and that it should be avoided to reduce interaction torques. With the Generalized Elasticities, interaction torques decrease further, and the human finally needs on average only about half the effort to move the exoskeleton.

The consequences of the interaction torques are visible in the walking cadence. When interaction torques are reduced, the cadence is closer to the value observed when walking without the robot, hinting that subjects might be able to match their own physiological pattern more closely.

The observation that foot clearance seems to be an issue with Generalize Elasticities may be due to the steepness of the force profile. The gradual behavior of gravity compensation might allow for motor adaptation of the human, whereas short force peaks are difficult to anticipate. Future work should take this into account by smoother force fields.

It should be noted that the method requires that preferred human motions are known in advance, at least approximately. If a subject deviates from the expected motion, compensation of the robot's dynamics is not optimal anymore. There may be cases where interaction torques increase due to the conservative force field, for example when actual motions are slow and the force field has been optimized for highly dynamic motions. One solution for this is to concatenate

many different trajectories for the optimization of the field, covering a large number of possible motions. Although the resulting force field will represent a compromise and the fit is not optimal anymore for each single movement, the generality improves. Another solution is to calculate various force fields for different motions, and to choose the appropriate one for a given situation. In the example of gait rehabilitation, very slow gait will require a different force field than faster gait. However, switching/blending between different force fields needs to be handled with care, due to a possible violation of passivity in time-variable control.

VI. CONCLUSION AND OUTLOOK

This paper presented the systematic method of Generalized Elasticities, which shapes optimal passive robot dynamics. Conservative force fields minimize undesired interaction forces/torques needed by the human to move the robot. The approach is easily applicable, as it does not require a model of the human, nor a similar kinematic structure of human and robot. Experiments with healthy subjects walking in the Lokomat lower extremity exoskeleton confirmed that interaction torques can be reduced by the proposed method. An observed consequence was that subject's gait resembled more closely their natural gait in terms of walking cadence. An important benefit can be that the modes of therapy available with current rehabilitation robots may be improved to allow more effective trainings.

Current work aims at better parameterizations, for example using Compactly Supported Radial Basis Functions to parameterize the potential instead of the force field, and at a unification of the transparency enhancement with other functionalities like support and guidance of the human [28].

ACKNOWLEDGMENTS

The authors would like to thank all subjects who participated in the evaluation. The contents of this publication were developed in part with support of the National Center of Competence in Research (NCCR) on Neural Plasticity and Repair of the Swiss National Science Foundation and in part under a grant from the US Department of Education, NIDRR grant number H133E070013. However, those contents do not necessarily represent the policy of the US Department of Education, and you should not assume endorsement by the Federal Government of the United States of America.

REFERENCES

- [1] A. H. A. Stienen, E. E. G. Hekman, F. C. T. Van der Helm, G. B. Prange, M. J. A. Jannink, A. M. M. Aalsma, and H. Van der Kooij. Dampace: dynamic force-coordination trainer for the upper extremities. In *Proc IEEE Int Conf Rehab Rob (ICORR)*, pp. 820–826. Noordwijk, the Netherlands, 2007.
- [2] T. Nef, M. Mihelj, and R. Riener. ARMin: a robot for patient-cooperative arm therapy. *Medical & Biological Engineering & Computing*, **45**(9):887–900, 2007.
- [3] J. F. Veneman, R. Ekkelenkamp, R. Kruidhof, F. van der Helm, and H. van der Kooij. A Series Elastic- and Bowden-Cable-Based Actuation System for Use as Torque Actuator in Exoskeleton-Type Robots. *Int J Rob Res*, **25**(3):261–281, 2006.
- [4] J. Pratt, B. Krupp, C. Morse, and S. Collins. The RoboKnee: An exoskeleton for enhancing strength and endurance during walking. In *Proc IEEE Int Conf Rob Aut (ICRA)*, pp. 2430–2435. 2004.
- [5] G. Colombo, M. Joerg, R. Schreier, and V. Dietz. Treadmill training of paraplegic patients using a robotic orthosis. *Journal of Rehabilitation Research and Development*, **37**(6):693–700, 2000.
- [6] S. Banala, S. Agrawal, and J. Scholz. Active Leg Exoskeleton (ALEX) for Gait Rehabilitation of Motor-Impaired Patients. In *Proc IEEE Int Conf Rehab Rob (ICORR)*, pp. 401–407. 2007.
- [7] D. Aoyagi, W. E. Ichinose, S. J. Harkema, D. J. Reinkensmeyer, and J. E. Bobrow. A robot and control algorithm that can synchronously assist in naturalistic motion during body-weight-supported gait training following neurologic injury. *IEEE Transactions on Neural Systems and Rehabilitation Engineering*, **15**(3):387–400, 2007.
- [8] N. Hogan, H. Krebs, J. Charnnarong, P. Srikrishna, and A. Sharon. MIT-MANUS: a workstation for manual therapy and training. I. In *Proc IEEE Int Worksh Rob Hum Comm (Ro-Man)*, pp. 161–165. 1992.
- [9] S. Hesse and D. Uhlenbrock. A Mechanized Gait Trainer for Restoration of Gait. *Journal of Rehabilitation Research and Development*, **37**(6):701–708, 2000.
- [10] H. Schmidt, S. Hesse, R. Bernhardt, and J. Krüger. HapticWalker - a novel haptic foot device. *ACM Transactions on Applied Perception*, **2**(2):166–180, 2005.
- [11] M. Peshkin, D. A. Brown, J. J. Santos-Munné, A. Makhlin, E. Lewis, J. E. Colgate, J. Patton, and D. Schwandt. KineAssist: A robotic overground gait and balance training device. In *Proc IEEE Int Conf Rehab Rob (ICORR)*, pp. 241–246. Chicago, 2005.
- [12] H. Kawamoto and S. Kanbe. Power Assist Method for HAL3, Estimating Operator Intention Based on Motion Information. In *Proc IEEE Int Worksh Rob Hum Comm (Ro-Man)*, pp. 67–72. 2003.
- [13] A. Chu, H. Kazerooni, and A. Zoss. On the Biomimetic Design of the Berkeley Lower Extremity Exoskeleton (BLEEX). In *Proc IEEE Int Conf Rob Aut (ICRA)*, pp. 4356–4363. 2005.
- [14] R. Riener, L. Lunenburger, S. Jezernik, M. Anderschitz, G. Colombo, and V. Dietz. Patient-cooperative strategies for robot-aided treadmill training: first experimental results. *IEEE Transactions on Neural Systems and Rehabilitation Engineering*, **13**:380–394, 2005.
- [15] J. L. Emken, R. Benitez, and D. J. Reinkensmeyer. Human-robot cooperative movement training: Learning a novel sensory motor transformation during walking with robotic assistance-as-needed. *Journal of NeuroEngineering and Rehabilitation*, **4**, 2007.
- [16] C. Fleischer. *Controlling Exoskeletons with EMG signals and a Biomechanical Body Model*. Ph.D. thesis, TU Berlin, 2007.
- [17] H. Vallery, E. van Asseldonk, M. Buss, and H. van der Kooij. Reference Trajectory Generation for Rehabilitation Robots: Complementary Limb Motion Estimation. *IEEE Transactions on Neural Systems and Rehabilitation Engineering*, **17**(1):23–30, 2009.
- [18] G. A. Pratt, M. M. Williamson, P. Dillworth, J. Pratt, K. Ulland, and A. Wright. Stiffness Isn't Everything. In *International Symposium on Experimental Robotics (ISER)*. 1995.
- [19] H. Vallery, J. Veneman, E. van Asseldonk, R. Ekkelenkamp, M. Buss, and H. van der Kooij. Compliant Actuation of Rehabilitation Robots - Benefits and Limitations of Series Elastic Actuators. *IEEE Robotics and Automation Magazine (RAM)*, **15**(3):60–69, 2008.
- [20] N. Hogan. Impedance control: An approach to manipulation. Part I - Theory, Part II - Implementation, Part III - Applications. *ASME J Dyn Sys Meas Con*, **107**:1–24, 1985.
- [21] E. Colgate and N. Hogan. An analysis of contact instability in terms of passive physical equivalents. In *Proc IEEE Int Conf Rob Aut (ICRA)*, pp. 404–409. Scottsdale, AZ, USA, 1989.
- [22] B. S. and O. Khatib (ed.). *Handbook of Robotics*. Springer, 2008.
- [23] E. Todorov. Optimality principles in sensorimotor control. *Nature Neuroscience*, **7**(9):907–915, 2004.
- [24] S. H. Collins, M. Wisse, and A. Ruina. A Three-Dimensional Passive-Dynamic Walking Robot with Two Legs and Knees. *The International Journal of Robotics Research*, **20**(7):607–615, 2001.
- [25] D. P. Ferris, K. E. Gordon, G. S. Sawicki, and A. Peethambaran. An improved powered ankle-foot orthosis using proportional myoelectric control. *Gait & Posture*, **23**(4):425–428, 2006.
- [26] A. J. van den Bogert. Exotendons for assistance of human locomotion. *Biomed Eng Online*, **2**:17, 2003.
- [27] A. Iske. *Multiresolution Methods in Scattered Data Modelling*. Lecture Notes in Comp Sc Eng. Springer-Verlag, Heidelberg, 2004.
- [28] H. Vallery, A. Duschau-Wicke, and R. Riener. Generalized Elasticities Improve Patient-Cooperative Control of Rehabilitation Robots. *Submitted for the IEEE Int Conf Rehab Rob (ICORR)*, 2009.